Mapping the Dark Side: Visual Selectivity of Default Network Deactivations

Tomas Knapen (tknapen@gmail.com)

Experimental and Applied Psychology, Vrije Universiteit Amsterdam
Van der Boechorststraat 1, 1081BT Amsterdam, the Netherlands
Spinoza Centre for Neuroimaging, Amsterdam, the Netherlands

Daan van Es (daan.van.es@gmail.com)

Experimental and Applied Psychology, Vrije Universiteit Amsterdam
Van der Boechorststraat 1, 1081BT Amsterdam, the Netherlands

Abstract

The brain's default network (DN) deactivates when participants focus externally to perform a task, and activates for internally referenced mental states such as mind wandering and autobiographical memory. Processing in the DN is thought to represent the highest levels of information integration, and changes to their responses are implicated in many psychological disorders. Recent findings indicate that signals in the DN carry visual memory information, but the functional role of DN deactivations in particular remains unclear. Here we show that BOLD signal decreases in the DN are tuned to the spatial location of visual stimuli. The visual selectivity of these deactivations was similar to that of concurrent activations in the frontal and parietal regions of the multiple demand network. Furthermore, visually selective deactivations allowed us to decode the location of a visual stimulus from DN nodes, demonstrating that the DN contains functional representations of the visual field. Our results indicate that responses in the DN are pinioned to responses in the visual system, providing a candidate organization for the mnemonic functionality of the DN. Our results suggest that the DN may utilize sensory reference frames for higher-level cognition such as autobiographical memory and social thought.

Keywords: population receptive field models, fMRI, default network, model-based decoding

Introduction

The Default Network encompasses around 40% of the human neocortical surface, and activates when a diverse set of high-level cognitive acts take place (Raichle, 2015). Among these are autobiographical memory, navigation, future planning, and social reasoning (Mars et al., 2012; Gerlach, Spreng, Madore, & Schacter, 2014; Spreng, Mar, & Kim, 2009; Fox, Foster, Kucyi, Daitch, & Parvizi, 2018). In accordance with this crucial role of DN function in high-level cognition, alterations in DN responses are implicated in a host of clinical disorders (Padmanabhan, Lynch, Schaer, & Menon, 2017; Pomarol-Clotet et al., 2008; Hafkemeijer, van der Grond, & Rombouts, 2012). Recent research shows that signals in the DN reflect neural mechanisms implementing visuomnemonic function (Sestieri, Shulman, & Corbetta, 2010; Lee, Chun, & Kuhl, 2016; Guerin, Robbins, Gilmore, & Schacter, 2012), but the computational structure implemented by the DN is unknown. We investigated this computational

structure by focusing on the well-documented deactivations that occur in the DN when participants focus on sensory information to perform a task (Raichle, 2015). We performed a visual mapping fMRI experiment at ultra-high field (7 Tesla) in which a bar-shaped stimulus systematically traversed the visual field in different directions.
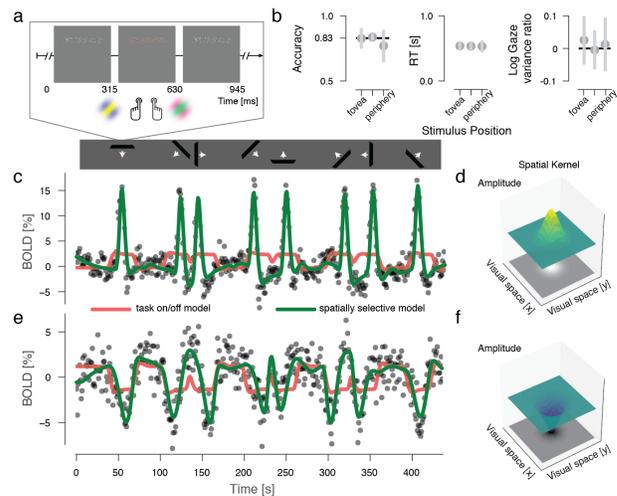
Figure 1: Behavior and single-voxel responses. a. Stimulus and task design. b. Behavioral results. There was no significant difference between accuracy, reaction time and gaze variability as a function of the bar stimulus locations. c-d. BOLD signal time-course from a single V1 voxel. This response is best explained by a spatially selective model (green line, implemented as spatially localized Gaussian kernel with a positive amplitude) than by a simple task on/off model (red line). e-f. BOLD signal time-course of a single angular gyrus voxel. Contrary to V1 responses, BOLD signals decreased when a stimulus was presented within the voxels pRF. This response is best explained by a spatially selective model (a Gaussian kernel with a negative amplitude, green line), rather than by the task on-off model.

Results

Participants performed a two-alternative forced-choice color discrimination task on the stimulus (Figure 1a) titrated to be equally demanding throughout the visual field (Figure 1b).
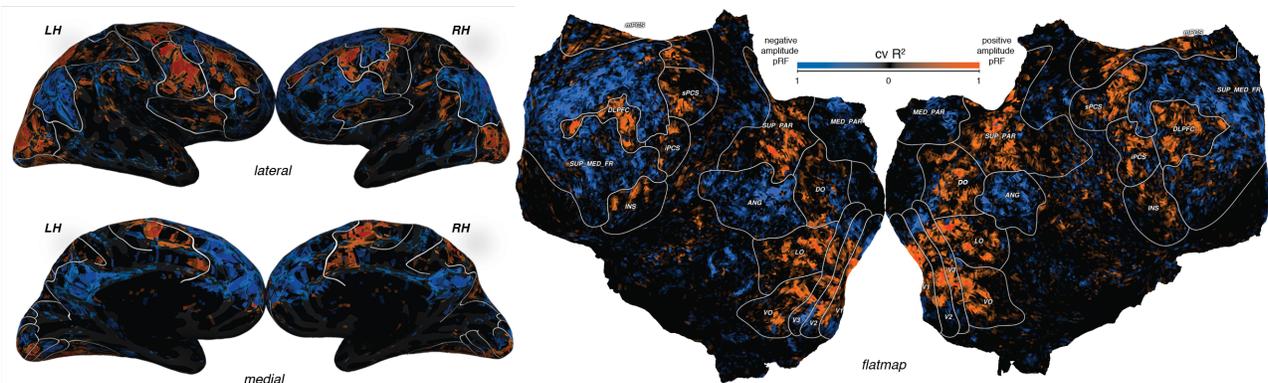
Figure 2: Inflated and flattened depictions of positive (red) and negative (blue) pRFs across the cortical surface of an example subject. VO: ventral occipital cortex encompassing visual field maps V4 and VO1/2; LO: lateral occipital cortex encompassing visual field maps LO1/2 and TO1/2; DO: dorsal occipital cortex encompassing visual field maps V3AB, V7 and IPS0/1; SUP_PAR: superior parietal lobe, encompassing visual field maps IPS2/3/4/5; sPCS: superior precentral sulcus; iPCS: inferior precentral sulcus; mPCS: medial precentral sulcus; DLPFC: dorsolateral prefrontal cortex; INS: insula; ANG: Angular Gyrus; MED_PAR: medial parietal lobe; SUP_MED_FR: superior & medial cortex.

Across participants, there was no difference in task performance ($F_{(2,10)} = 1.347$, $p = .304$, $\eta^2 = .198$) or reaction time ($F_{(2,10)} = 0.121$, $p = .887$, $\eta^2 = .003$) for different locations of the visual stimulus. In addition, we verified that the bar stimulus did not induce eye movements, as the variability in gaze direction did not depend on the direction of the visual stimulus ($F_{(1,10)} = 0.222$, $p = .657$, $\eta^2 = .018$), for all bar stimulus eccentricities. These results show that task difficulty and attentional load did not change as a function of stimulus location and rule out the possibility of confounding task-related signals with spatially selective signals. Turning to the recorded BOLD responses, Figure 1c shows the time-course of visual stimulation and the resulting BOLD fluctuations from a single cortical location in primary visual cortex. As expected in this brain region, the structured visual input caused BOLD increases only when the stimulus was present within a circumscribed region of the visual field (see Figure 1d), mathematically modeled as a population receptive field (pRF) (Dumoulin & Wandell, 2008; Dumoulin & Knapen, 2018). This spatially selective model shows an excellent approximation to the BOLD signal time-courses (across-runs average cross-validated (CV) $R^2 = 0.82$), compared to a model that has no visual field selectivity and only encodes stimulus/task presence (CV $R^2 = 0.10$). We then applied identical analyses to BOLD signals arising in the DN, from the same recordings. Figure 1e shows an example signal time-course from the lateral parietal angular gyrus and illustrates the strong BOLD signal decreases observed whenever a stimulus was presented. Our spatially non-selective model fit the deactivations of this cortical location during stimulus presence (CV $R^2 = 0.15$), confirming that it is not only anatomically but also functionally part of the DN. However, the strongest deactivations are not captured by this spatially non-selective model. We therefore fit a spatially selective model

that implements a negative population receptive field (Figure 1f). This model captures the specific temporal structure of deactivations, showing much better cross-validated prediction performance than the spatially non-selective model (CV $R^2 = 0.63$). These results indicate that DN negative BOLD responses encode visual location, which can be computationally formalised as a spatial pRF of negative amplitude. This pattern of results was typical for recordings from the DN, and we selected only voxels where the spatially selective model outperformed the non-selective model for further analysis. Figure 2 shows inflated and flattened cortical surface depictions of the predictive power of our spatially selective model, colored based on whether they result from activations (orange colormap) or deactivations (blue colormap). The spatial distribution of activations across the cortical surface confirms earlier findings of visual selectivity in parietal and frontal cortex (Swisher, Halko, Merabet, McMains, & Somers, 2007; Mackey, Winawer, & Curtis, 2017). The spatial distribution of deactivations on the other hand corresponds well with the locations of DN nodes in parietal and frontal brain regions as found in resting-state experiments which used large populations of participants (Glasser, Coalson, Robinson, & Hacker, 2015; Yeo et al., 2011). Across participants, there was some variability in the exact locations of the clusters of negative pRFs. These individual-level specificities of deactivations are reminiscent of recent findings showing fine-grained connectivity between DN nodes (Braga & Buckner, 2017). Having shown that cortical locations in the DN represent visual field locations, we then asked if the pattern of deactivations within separate DN nodes encodes the location of a stimulus in the visual field (Figure 3). Specifically, we used pRF parameter estimates from a given cortical region as an explicit encoding model. We then used a recently developed Bayesian decoding algorithm (van Bergen, Ma, Pratte, & Je-

hee, 2015) to calculate the most probable stimulus pattern given the structure of BOLD responses across voxels in a test dataset, separately for every TR (Figure 3a). Performing this analysis results in movies of inferred stimulus representations for the entire experiment (Figure 3b-c). We quantified the fidelity of a brain regions representation of visual field location of a stimulus by means of the correlation between the actual stimulus location and the inferred stimulus location. Figure 3d shows that stimulus position can be decoded from known parietal and frontal retinotopic areas (two-tailed t-test on median across CV folds, sPCS: t(5)=5.48, p=0.003, iPCS: t(5)=4.13, p=0.009, SUP_PAR: t(5)=6.86, p=0.001), reflecting their visuospatial organization. The same analysis, performed on DN nodes, found significant correlations between actual and decoded stimulus position (ANG: t(5)=4.80, p=0.005, MED_PAR: t(5)=3.264, p=0.022, SUP_MED_FR: t(5)=4.13, p=0.009, Figure 3e). In sum, we find significant decoding performance for DN nodes with a fidelity similar to that of known retinotopic regions in higher-level visual cortex (Figure 3f).

Discussion

These results indicate that DN areas encode relatively detailed visual location information by means of their deactivations. The DN is thought to constitute one extreme of a gradient leading from primary sensory and motor regions to transmodal association cortex (Buckner & Krienen, 2013; Margulies et al., 2016). What would be the use of the brain representing visual location in these high-level regions that integrate across sensory modalities? We offer two potential and non-exclusive computational roles for this neural signature. First, the signal increases of these DN regions in memory (Sestieri, Shulman, & Corbetta, 2017) and social semantic information processing (Huth, de Heer, Griffiths, Theunissen, & Gallant, 2016) indicate that the DN activates for computations that emphasize internally instead of externally oriented information processing. The balance between the multiple demand and default networks could serve to tune processing either outwards or inwards, i.e. towards incident sensory information or, conversely, towards memory-based and/or ego-referenced processing. Our results suggest that sensory space, and visual space in particular, could serve as a shared reference frame for this interaction between networks. Second, there is abundant evidence from sensory processing that the interplay between activations and deactivations can serve to decorrelate neural responses to input patterns (Barlow, 1961) and increase processing efficiency by means of predictive coding (Srinivasan, Laughlin, & Dubs, 1982). Especially in the matching of multiple input patterns there is inherent computational benefit to representing what is not there, as opposed to solely representing what is there (Goncalves & Welchman, 2017). The DN is ideally suited to perform this type of matching operation on the level of transmodal association (Margulies et al., 2016) and memory (Sestieri et al., 2017). Our results suggest that the spatial arrangement of
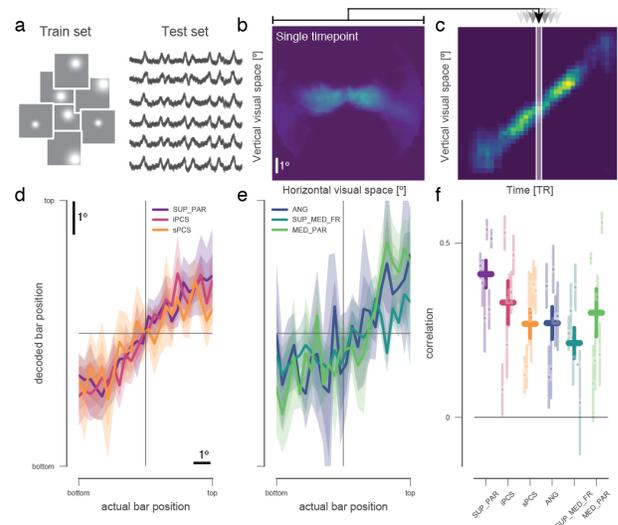
Figure 3: Decoding of visual location. Using a forward model, we decoded the location of our visual stimulus in a cross-validated fashion. a. pRF fits from a training set were combined with voxel time-series from an independent test set. b. We computed the most likely spatial stimulation based on the pattern of voxel responses on every time point, example from visual area V2. c. These images were then rotated relative to the bars direction, averaged first across stimulus directions, and then across the direction perpendicular to the stimulus. The center of mass of the resulting spatial distribution for each timepoint was taken as the decoded bar position (after shifting by the haemodynamic delay of the BOLD response). d. Known high-level retinotopic maps in parietal and frontal cortex show a strong correlation between actual and decoded stimulus position. e. DN regions allow decoding of visual stimulus location based on their BOLD signal decreases. f. Decoding results across regions and participants. Error bars represent the standard error of the mean across participants and CV folds.

sensory inputs may be inherited by the DN to frugally support higher-level cognition.

References

Barlow, H. B. (1961). *Possible principles underlying the transformations of sensory messages.*

Braga, R. M., & Buckner, R. L. (2017, July). Parallel Inter-digitated Distributed Networks within the Individual Estimated by Intrinsic Functional Connectivity. *Neuron*, *95*(2), 457–471.e5.

Buckner, R. L., & Krienen, F. M. (2013, December). The evolution of distributed association networks in the human brain. *Trends in cognitive sciences*, *17*(12), 648–665.

Dumoulin, S. O., & Knapen, T. H. J. (2018). How Visual Cortical Organization Is Altered by Ophthalmologic and Neurologic Disorders. *Annual Review of Vision Science*, *in press*.

Dumoulin, S. O., & Wandell, B. A. (2008, January). Population receptive field estimates in human visual cortex. *NeuroImage*, *39*(2), 647–660.

Fox, K. C. R., Foster, B. L., Kucyi, A., Daitch, A. L., & Parvizi, J. (2018, April). Intracranial Electrophysiology of the Human Default Network. *Trends in cognitive sciences*, *22*(4), 307–324.

Gerlach, K. D., Spreng, R. N., Madore, K. P., & Schacter, D. L. (2014, December). Future planning: default network activity couples with frontoparietal control network and reward-processing regions during process and outcome simulations. *Social cognitive and affective neuroscience*, *9*(12), 1942–1951.

Glasser, M. F., Coalson, T., Robinson, E., & Hacker, C. (2015). A Multi-modal parcellation of human cerebral cortex. *Nature*, *80*, 18–26.

Goncalves, N. R., & Welchman, A. E. (2017, May). "What Not" Detectors Help the Brain See in Depth. *Current biology : CB*, *27*(10), 1403–1412.e8.

Guerin, S. A., Robbins, C. A., Gilmore, A. W., & Schacter, D. L. (2012, September). Interactions between Visual Attention and Episodic Retrieval: Dissociable Contributions of Parietal Regions during Gist-Based False Recognition. *Neuron*, *75*(6), 1122–1134.

Hafkemeijer, A., van der Grond, J., & Rombouts, S. A. R. B. (2012, March). Imaging the default mode network in aging and dementia. *Biochimica et biophysica acta*, *1822*(3), 431–441.

Huth, A. G., de Heer, W. A., Griffiths, T. L., Theunissen, F. E., & Gallant, J. L. (2016, April). Natural speech reveals the semantic maps that tile human cerebral cortex. *Nature*, *532*(7600), 453–458.

Lee, H., Chun, M. M., & Kuhl, B. A. (2016). Lower parietal encoding activation is associated with sharper information and better memory. *Cerebral Cortex*.

Mackey, W. E., Winawer, J., & Curtis, C. E. (2017, June). Visual field map clusters in human frontoparietal cortex. *eLife*, *6*, 2704.

Margulies, D. S., Ghosh, S. S., Goulas, A., Falkiewicz, M., Huntenburg, J. M., Langs, G., ... Smallwood, J. (2016, November). Situating the default-mode network along a principal gradient of macroscale cortical organization. *Proceedings of the National Academy of Sciences of the United States of America*, *113*(44), 12574–12579.

Mars, R. B., Neubert, F.-X., Noonan, M. P., Sallet, J., Toni, I., & Rushworth, M. F. S. (2012). On the relationship between the "default mode network" and the "social brain". *Frontiers in Human Neuroscience*, *6*, 189.

Padmanabhan, A., Lynch, C. J., Schaer, M., & Menon, V. (2017, September). The Default Mode Network in Autism. *Biological Psychiatry: Cognitive Neuroscience and Neuroimaging*, *2*(6), 476–486.

Pomarol-Clotet, E., Salvador, R., Sarró, S., Gomar, J., Vila, F., Martínez, A., ... McKenna, P. J. (2008, August). Failure to deactivate in the prefrontal cortex in schizophrenia: dysfunction of the default mode network? *Psychological medicine*, *38*(8), 1185–1193.

Raichle, M. E. (2015, July). The brain's default mode network. *Annual review of neuroscience*, *38*(1), 433–447.

Sestieri, C., Shulman, G. L., & Corbetta, M. (2010, June). Attention to memory and the environment: functional specialization and dynamic competition in human posterior parietal cortex. *The Journal of neuroscience : the official journal of the Society for Neuroscience*, *30*(25), 8445–8456.

Sestieri, C., Shulman, G. L., & Corbetta, M. (2017, March). The contribution of the human posterior parietal cortex to episodic memory. *Nature Reviews Neuroscience*, *18*(3), 183–192.

Spreng, R. N., Mar, R. A., & Kim, A. S. N. (2009, March). The common neural basis of autobiographical memory, prospection, navigation, theory of mind, and the default mode: a quantitative meta-analysis. *Journal of Cognitive Neuroscience*, *21*(3), 489–510.

Srinivasan, M. V., Laughlin, S. B., & Dubs, A. (1982, November). Predictive coding: a fresh view of inhibition in the retina. *Proceedings of the Royal Society of London Series B, Containing papers of a Biological character Royal Society (Great Britain)*, *216*(1205), 427–459.

Swisher, J. D., Halko, M. A., Merabet, L. B., McMains, S. A., & Somers, D. C. (2007, May). Visual topography of human intraparietal sulcus. *The Journal of neuroscience : the official journal of the Society for Neuroscience*, *27*(20), 5326–5337.

van Bergen, R. S., Ma, W. J., Pratte, M. S., & Jehee, J. F. M. (2015, December). Sensory uncertainty decoded from visual cortex predicts behavior. *Nature Neuroscience*, *18*(12), 1728–1730.

Yeo, B. T. T., Krienen, F. M., Sepulcre, J., Sabuncu, M. R., Lashkari, D., Hollinshead, M., ... Buckner, R. L. (2011, September). The organization of the human cerebral cortex estimated by intrinsic functional connectivity. *Journal of Neurophysiology*, *106*(3), 1125–1165.